



Virginia Commonwealth University  
VCU Scholars Compass

---

Biology and Medicine Through Mathematics  
Conference

2022

---

May 20th, 11:00 AM - 11:30 AM

## Mechanical Parameters Fitting for Layer-reduced Umbilical Arteries Used for Grafting

Kun Gou

*Texas A&M University-San Antonio*, [kgou@tamusa.edu](mailto:kgou@tamusa.edu)

Follow this and additional works at: <https://scholarscompass.vcu.edu/bamm>

 Part of the [Life Sciences Commons](#), [Medicine and Health Sciences Commons](#), and the [Physical Sciences and Mathematics Commons](#)

---

<https://scholarscompass.vcu.edu/bamm/2022/fri/10>

This Event is brought to you for free and open access by the Dept. of Mathematics and Applied Mathematics at VCU Scholars Compass. It has been accepted for inclusion in Biology and Medicine Through Mathematics Conference by an authorized administrator of VCU Scholars Compass. For more information, please contact [libcompass@vcu.edu](mailto:libcompass@vcu.edu).

# Mechanical Parameters Fitting for Layer-reduced Umbilical Arteries Used for Grafting

Rene Alvarado, Kun Gou\*

## Abstract

The umbilical artery (UA) functions to carry deoxygenated blood from the fetus to the placenta during pregnancy. It is discovered that this artery can be used as an efficient by-pass graft to repair the occluded or narrowed coronary artery for other patients to restore normal blood flow [1, 2]. The outer layer of the UA is usually removed to get rid of the immunogenic cellular components in the UA to minimize the immune cells' biological activities on the extracellular matrix for the UA's better adaptation to the patient's coronary artery [3]. The stiffness of the layer-reduced UA is different from the original UA, and is difficult to measure directly by lab experiments due to its cylindrical shape. However, understanding stiffness of the bypass graft is important to predict how it can successfully adapt to the patient's coronary artery for normal functionality [4]. This study aims at establishing proper mathematical models and employing numerical optimization techniques to obtain the stiffness parameters of the layer-reduced UA based on lab measurements. The artery wall is considered to be of hyperelastic soft tissue [5] incorporated with two families of fibers. An objective function is established employing the difference between the theoretical and lab results. Minimization of the objective function then provides the shear modulus of the isotropic matrix and the fiber stiffness and orientation parameters.

## 1 Constitutive modeling

The reference configuration of the UA is unloaded with traction-free inner and outer boundary conditions. We also ignore the residual stress in this unloaded configuration due to experimental observation of no obvious opening angle when cutting the UA radially. Under the loaded, deformed configuration, the UA is subject to an inner pressure  $P$  in the inflating experiments (Fig. 1). The UA is nearly cylindrical. We thus set up the model under the cylindrical coordinate system [6]. The coordinates in the radial, angular, and axial directions are expressed by  $(R, \Theta, Z)$  in the reference configuration, and the corresponding coordinates in the deformed configuration are expressed by the related lower case letters  $(r, \theta, z)$ . The basis vectors for the cylindrical coordinates in the reference and deformed configurations are, respectively, “ $\mathbf{e}_R, \mathbf{e}_\Theta, \mathbf{e}_Z$ ”, and “ $\mathbf{e}_r, \mathbf{e}_\theta, \mathbf{e}_z$ ”.

The mapping from the reference configuration to the deformed configuration is expressed as  $r = r(R), \theta = \Theta, z = \lambda_z Z$ , where  $r(R)$  is the radial function, and  $\lambda_z$  is the axial stretch ratio. The deformation gradient  $\mathbf{F}$  is thus  $\mathbf{F} = r'(R)\mathbf{e}_r \otimes \mathbf{e}_R + \frac{r}{R}\mathbf{e}_\theta \otimes \mathbf{e}_\Theta + \lambda_z \mathbf{e}_z \otimes \mathbf{e}_Z$ . The right Cauchy-Green tensor  $\mathbf{C}$  satisfying  $\mathbf{C} = \mathbf{F}^T \mathbf{F}$ , generating the first invariant  $I_1 = \text{tr} \mathbf{C}$ . We further assume that the volume of the arterial segment is preserved during the mapping from the reference configuration to the deformed configuration satisfying  $\det \mathbf{F} = 1$ .

Two symmetric families of fibers are oriented in the wall. The unit direction vectors for these fiber families are  $\mathbf{N}^{(1)} = \sin \varphi \mathbf{e}_\Theta + \cos \varphi \mathbf{e}_Z$ , and  $\mathbf{N}^{(2)} = -\sin \varphi \mathbf{e}_\Theta + \cos \varphi \mathbf{e}_Z$ , where  $\varphi$  is the acute angle between the fiber unit direction vector and the axial axis. These oriented fibers contribute strain energy to the UA. We take the fiber strain-energy density functions [7] to be

$$W_f = \frac{k_1}{2k_2} \sum_{n=1}^2 \left[ e^{k_2 E_n^2} - 1 \right] \quad \text{with} \quad E_n = \kappa I_1 + (1 - 3\kappa) I_4^{(n)} - 1, \quad (1)$$

---

\*Authors' address: Texas A&M University-San Antonio, Department of Mathematical, Physical, and Engineering Sciences, One University Way, San Antonio, Texas 78224. Rene Alvarado was a junior undergraduate student in the mathematics major at the time of article publication. Corresponding author: Dr. Kun Gou; email: kgou@tamusa.edu.

where  $k_1$ ,  $k_2$ , and  $\kappa$  in (1) are parameters for fibers in the wall. The pseudo-invariant  $I_4^{(n)}$  ( $n=1, 2$ ) for the two families of fibers is defined as  $I_4^{(n)} = \mathbf{N}^{(n)} \cdot \mathbf{C}\mathbf{N}^{(n)}$  [8]. The wall consists of elastic groundmatrix and the two families of fibers. We take the elastin groundmatrix contributed strain-energy density function to be in the form of a neo-Hookean model  $W_e = \frac{\mu}{2}(I_1 - 3)$ , where  $\mu$  is the shear modulus of the groundmatrix. The total strain-energy density function is  $W = W_e + W_f$ .

For the incompressible hyperelastic material, the Cauchy stress tensor  $\mathbf{T}$  is derived from the strain energy density function  $W$  via the formula  $\mathbf{T} = -p\mathbf{I} + 2\mathbf{F}\frac{\partial W}{\partial \mathbf{C}}\mathbf{F}^T$ , where  $p$  is a constraint parameter needing determination, and  $\mathbf{I}$  is the identity tensor. The Cauchy stress components in the radial, circumferential, and axial directions are expressed by  $T_{rr}$ ,  $T_{\theta\theta}$ , and  $T_{zz}$ , respectively. The Cauchy stress tensor  $\mathbf{T}$  in a static state with gravity ignored for the light UA tissue satisfies the equation  $\text{div } \mathbf{T} = \mathbf{0}$ , where ‘‘div’’ represents divergence of the related quantity. The inner boundary ( $R = R_{in}$ ) of the UA is subjected to the pressure in the vector form  $P\mathbf{e}_r$  with  $P > 0$ , by which we obtain  $T_{rr}|_{R=R_{in}} = -P$ . Over the outer boundary ( $R = R_{out}$ ), the radial Cauchy stress is 0, and we have  $T_{rr}|_{R=R_{out}} = 0$ .

## 2 Parameters fitting

The inflating experimental design is illustrated in Fig. 1. The left end is subject to a pressure  $P$ . We denote the inner boundary radius of the inflated UA to be  $r_{in}$ , and the outer boundary radius of the inflated UA to be  $r_{out}$ . The right end is closed with a total force  $L$  imposed on the UA. The force generated by  $T_{zz}$  to the left end of the UA, the force generated by the left pressure to the UA, and the force  $L$  on the right end satisfy the force equilibrium equation

$$2\pi \int_{r_{in}}^{r_{out}} T_{zz} r dr - P\pi r_{in}^2 - L = 0. \quad (2)$$

The experiments recorded values of pressure  $P$ , the inner radius of the pressurized UA  $r_{in}$ , the outer radius of the pressurized UA  $r_{out}$ , the axial Cauchy stress value  $T_{zz}$ , the circumferential Cauchy stress value  $T_{\theta\theta}$ , and the force at the closed end  $L$ . We define the objective function for minimization to be

$$f = \sum_{k=1}^m (\omega_L |L_{the}^k - L_{lab}^k| + \omega_P |P_{the}^k - P_{lab}^k|), \quad (3)$$

where  $m$  is the number of equilibrium experiments performed,  $L_{the}^k$  and  $L_{lab}^k$  are the force values for  $L$  from the theoretical models and the lab experiments, respectively, and  $P_{the}^k$  and  $P_{lab}^k$  are the pressure values  $P$  from the theoretical models and the experiments, respectively. The quantities  $\omega_L (= 1)$  and  $\omega_P (= 200)$  are weights for the corresponding terms. The measured radii of the inner and outer boundaries of the UA are used as input in the model. We use the optimization toolboxes of Matlab for the layer-reduced UA to obtain parameters  $\mu$ ,  $\varphi$ ,  $\kappa$ ,  $\kappa_1$ , and  $\kappa_2$ .

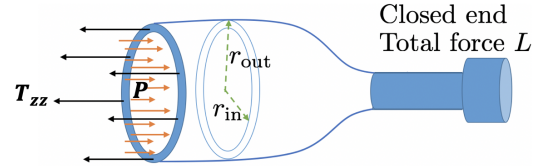


Figure 1: Simple illustration of the inflated arterial wall. The wall is closed on the right end with a total force  $L$  imposed over the wall. The left end is subject to the pressure  $P$ . The axial Cauchy stress on the left end of the inflated wall is  $T_{zz}$ . The inflated inner radius and outer radius of the wall are denoted by  $r_{in}$  and  $r_{out}$ , respectively.

### 2.1 Results and discussions

We study one sample of the UA. Over the traction-free configuration ( $P = 0$ ), the layer-reduced UA shows measure of  $r_{in} = 1.02$  mm and  $r_{out} = 1.14$  mm. Minimization of the objective function (3) generates the parameter values:  $\mu = 36.24$  kPa,  $\kappa_1 = 142.41$  kPa,  $\kappa_2 = 81.82$ ,  $\kappa = 0.30$ ,  $\varphi = 1.45$  radians. These parameter results are subjected to change for different UA samples, different objective functions, and even different initial input in the optimization [9]. In this short conference proceeding paper, we skip the other fitting results. Average of all these different values for each parameter can generate a more accurate value for that parameter. Statistical methods can be used to find a confidence interval for each parameter under fitting with a specified confidence level. This confidence interval can

provide a fundamental understanding how broadly each parameter may vary. Determination of the layer-reduced UA stiffness critically facilitates prediction of compatibility and efficiency of the bypass graft as a substitute coronary artery section for regular blood transport [10]. Our study applies mathematical models to fit the stiffness parameters based on experimental data, and resolves the difficulty of obtaining the mechanical parameters experimentally in the lab.

## References

- [1] Gui L, Mutu A, Chan SA, Breuer CK, Niklason LE. Development of decellularized human umbilical arteries as small-diameter vascular grafts. *Tissue Eng Part A*. 2009;15:2665–2676.
- [2] Victor RE, Brenda MG, Alejandro QG, Cynthia-Guadalupe RH, David FV, Oscar GZ, et al. Human umbilical vessels: Choosing the optimal decellularization method. *Asaio J*. 2018;64:575–580.
- [3] Youngstrom DW, Barrett JG, Jose RR, Kaplan DL. Functional characterization of detergent-decellularized equine tendon extracellular matrix for tissue engineering applications. *PLoS One*. 2013;8:e64151.
- [4] Owens CD, Wake N, Jacot JG, Gerhard-Herman M, Gaccione P, Belkin M, et al. Early biomechanical changes in lower extremity vein grafts—distinct temporal phases of remodeling and wall stiffness. *J Vasc Surg*. 2006;44:740–746.
- [5] Gou K, Baek S, Lutnesky MMF, Han HC. Growth-profile configuration for specific deformations of tubular organs: A study of growth-induced thinning and dilation of the human cervix. *PLoS ONE*. 2021;16:e0255895.
- [6] Gou K, Muddamallappa M. An analytic study on nonlinear radius change for hyperelastic tubular organs under volume expansion. *Acta Mech*. 2020;231:1503–1517.
- [7] Gasser TC, Ogden RW, Holzapfel GA. Hyperelastic modelling of arterial layers with distributed collagen fibre orientations. *J R Soc Interface*. 2006;3:15–35.
- [8] Gou K, Fok PW, Fu Y. Nonlinear tubular organ modeling and analysis for tracheal angioedema by swelling-morphoelasticity. *J Eng Math*. 2018;12:95–117.
- [9] Hu JJ, Baek S, Humphrey JD. Stress–strain behavior of the passive basilar artery in normotension and hypertension. *J Biomech*. 2007;40:2559–2563.
- [10] Hu JJ. Constitutive modeling of an electrospun tubular scaffold used for vascular tissue engineering. *Biomech Model Mechanobiol*. 2015;14:897–913.